Two-dimensional models of layered protoplanetary discs – II. The effect of a residual viscosity in the dead zone

R. Wünsch,[1,3]★ A. Gawryszczak,[1] H. Klahr[2] and M. Różyczka[1]

[1]*Nicolaus Copernicus Astronomical Center, Bartycka 18, 00-716 Warsaw, Poland*
[2]*Max-Planck-Institut für Astronomie, Königstuhl 17, 69117 Heidelberg, Germany*
[3]*Astronomical Institute, Academy of Sciences of the Czech Republic, Boční II 1401, 141 31 Prague, Czech Republic*

ABSTRACT

We study axisymmetric models of layered protoplanetary discs taking radiative transfer effects into account, and allowing for a residual viscosity in the dead zone. We also explore the effect of different viscosity prescriptions. In addition to the ring instability reported in the first paper of the series, we find an oscillatory instability of the dead zone, accompanied by variations of the accretion rate onto the central star. We provide a simplified analytical description explaining the mechanism of the oscillations. Finally, we find that the residual viscosity enables stationary accretion in large regions of layered discs. Based on results obtained with the help of a simple one-dimensional hydrocode, we identify these regions, and discuss conditions in which layered discs can give rise to FU Ori phenomena.

Key words: accretion discs – hydrodynamics – instabilities – Solar system: formation.

1 INTRODUCTION

The transport of angular momentum in protoplanetary discs is most probably driven by the magnetorotational instability, described by Balbus & Hawley (1991a,b), and hereafter referred to as MRI. Since the protoplanetary discs are ionized rather weakly, in some regions of the disc the ionization degree ξ can decrease below a critical level, ξ_c, at which the gas decouples from the magnetic field and the MRI decays. Such a region is referred to as a *dead zone*, contrary to the so-called *active zone* where the MRI operates.

The most important processes responsible for the ionization of a gas in protoplanetary discs are (1) particle collisions due to thermal motions, and (2) irradiation by cosmic rays and high-energy photons originating from the central star. The collisional ionization dominates in the innermost part of the disc, where the temperature is high enough to maintain $\xi > \xi_c$ at all distances from the disc plane. Further away from the star ξ_c is exceeded only in two surface layers (on both sides of the disc), each ionized by cosmic rays and stellar X-ray quanta, and having approximately constant column density Σ_a. Both processes result in the following distribution of disc activity: at $r < r_1$ (where the thermal ionization degree exceeds ξ_c) the whole disc is active; at $r_1 < r < r_2$ (where $\Sigma > \Sigma_a$) a dead zone is sandwiched between two active layers and at $r > r_2$ (where $\Sigma < \Sigma_a$) the whole disc becomes active again. This model was proposed by Gammie (1996) to explain the FU Ori outbursts.

FU Ori stars are young stellar objects whose optical brightness occasionally increases by 3–4 mag on a time-scale of 1–10 yr, and

remains at the increased level for 10–100 yr. It is generally believed that these events are related to the variations of the accretion rate in circumstellar discs. To explain the observed increase in luminosities, the accretion rate has to change from $\sim 10^{-7}$ to $\sim 10^{-4}\,M_\odot\,\mathrm{yr}^{-1}$, implying that as much as $10^{-2}\,M_\odot$ must be accreted onto the central star during the outburst (Hartmann & Kenyon 1996).

The FU Ori phenomenon may be caused by a thermal instability of the protoplanetary disc (see e.g. Bell & Lin 1994; Lodato & Clarke 2004 and references therein), analogous to the one operating in accretion discs around primary components of cataclysmic binaries (Meyer & Meyer-Hofmeister 1981). However, the thermal instability model has difficulties with explaining long duration of the outbursts, since the high accretion rate during the outburst quickly removes most of the material from the inner part of the disc where the instability occurs (Hartmann & Kenyon 1996). A transition of the very inner disc to the outburst state due to the thermal instability was studied by Kley & Lin (1999) with the help of a similar two-dimensional (2D) code used in this work.

Gammie (1996) suggested that this problem may be solved by the layered model, in which the dead zone serves as a mass reservoir for the outburst. In the layered disc the accretion rate can be an increasing function of r. When this is the case, an annulus centred at r_0 receives more mass per unit time from the disc exterior to it ($r > r_0$) than it loses to the disc interior to it ($r < r_0$), causing the matter to accumulate in the dead zone. If this process lasts long enough, the total surface density of the disc may become so large that once the accretion was somehow triggered in the dead zone it would release enough heat to restore the coupling between the matter and the magnetic field. Such an 'ignition' of the accumulated matter

★E-mail: richard.wunsch@matfyz.cz

would then start a self-sustaining outflow of mas from the dead zone into the inner disc, substantially increasing the accretion rate.

Armitage, Livio & Pringle (2001) assume that the triggering factor is the gravitational instability. Their model shows repeating periods of vigorous accretion separated by quiescent intervals lasting $\sim 10^5$ yr, in qualitative agreement with the observed properties of FU Ori objects. However, our radiation-hydrodynamic simulations of layered discs (Wünsch, Klahr & Różyczka 2005, hereafter Paper I) indicate that it may be rather difficult for the dead zone to store $\sim 10^{-2}$ M$_\odot$ of the disc matter necessary to feed an FU Ori outburst. The reason is the ring instability described in Paper I, which, long before the required mass is reached, causes the dead zone to split into well-defined rings that become unstable to the instability discovered by Papaloizou & Pringle (1985).

In the present paper, we extend the simulations reported in Paper I onto a broader range of disc parameters, with the principal aim to find in which conditions the dead zone could become massive enough to account for FU Ori outbursts. For reasons explained in Section 2, along with models whose dead zones are entirely free of viscosity, we explore models with some residual viscosity acting in the region which formally should be declared dead. We also explore the effect of different viscosity prescriptions.

The paper is organized as follows. In Section 2, we briefly describe the numerical methods and input physics. The results of simulations are reported in Section 3. In Section 4, we give a simple analytical description of processes at the inner boundary of the dead zone, and derive conditions for ignition. In Section 5, we summarize our results and discuss the limits of the mass-accumulation process.

2 NUMERICAL METHODS AND INPUT PHYSICS

As in Paper I, the simulations are performed in spherical coordinates with the help of the radiation-hydrodynamics code TRAMP (Klahr, Henning & Kley 1999). The models are axially symmetric, but we do not impose an additional mirror symmetry with respect to the mid-plane of the disc, i.e. we allow for the flow through the mid-plane. Further technical details, such as boundary conditions or initialization procedure, can be found in Paper I.

The viscosity is treated according to the α-prescription of Shakura & Sunyaev (1973). In Paper I, following the argument that the turbulent viscosity coefficient should be proportional to the product of sound speed and the largest scale available for the turbulent eddies, we used the formula

$$\nu = \alpha c_{s,i} H_a, \tag{1}$$

where H_a is the half-thickness of the active layer, $c_{s,i}$ is the sound speed at the bottom of the active layer and α is a dimensionless parameter discussed below. In the present work this formula is employed in Models 1–3. The remaining models are obtained based on an alternative formula which allows for variations of ν with the distance from the mid-plane:

$$\nu = \alpha \frac{c_s^2}{\Omega}, \tag{2}$$

where c_s and Ω are *local* values of sound speed and angular velocity. Obviously, in a vertically averaged approximation assuming the zero-thickness dead zone both prescriptions are equivalent; however, in 2D models with the dead zone, we found that the details of the evolution are sensitive to the particular form of the viscosity formula (see Section 3).

We assume that at $T > T_{lim} = 1000$ K the ionization degree is high enough for the magnetorotational instability to operate and provide the source of viscosity, whereas at $T < T_{lim}$ the MRI is quenched. This assumption is based on the fact that at $T \sim 1000$ K ξ increases by five orders of magnitude due to ionization of potassium (Umebayashi 1983). Further, based on the cosmic ray stopping depth calculated by Umebayashi & Nakano (1981), we assume that on both sides of the disc a surface layer of column density $\Sigma_a = 100$ g cm^{-2} is made active due to ionization by energetic particles of cosmic origin.

In principle, ionization due to X-rays from the central star should also be taken into account. However, the corresponding active surface layer is probably not thicker than a few tens of g cm^{-2} (Glassgold, Najita & Igea 1997). The X-rays become important when the disc is screened from cosmic rays by magnetized stellar winds (Glassgold et al. 1997; Fromang, Terquem & Balbus 2002). In such cases, the ionization structure of the disc strongly depends on various model parameters such as properties of the X-ray source, critical magnetic Reynolds number or abundance of heavy metals (Fromang et al. 2002), and it is not possible to define one critical Σ_a for all possible circumstances. Unfortunately, such effects are too complicated to take them into account in multidimensional simulations, and an active surface layer of constant column density must serve as the necessary approximation. In effect, to define the boundary of the dead zone, we employ the simple model of disc ionization structure introduced by Gammie (1996).

In Paper I, α was set to 0 within the dead zone. However, it has been recently argued that the dead zone is not entirely dead in the sense that a residual viscosity can be maintained there by a purely hydrodynamic turbulence, excited by the non-axisymmetric waves propagating from the MRI-turbulent active layers (Fleming & Stone 2003). Following those arguments, in some models we allow for $\alpha_{DZ} \neq 0$. However, in all models the dead zone is much less viscous than the active zone, i.e. $\alpha_{DZ} \ll \alpha_a$.

In the previous work, we neglected the transport of heat by microturbulence, i.e. the heat was transported across the disc by radiation only. The same approximation is adopted here. While it would be poorly justified in one-dimensional (1D) models (see e.g. Cannizzo 2001), it is entirely reasonable in 2D discs, where the most important (i.e. the largest) turbulent scales are automatically taken into account, as they are resolved on the grid. Based on the similarity of the turbulence maintained by the magnetorotational instability to Kolmogoroff turbulence (Hawley, Gammie & Balbus 1995; Stone et al. 1996), we estimated that the subgrid microturbulent flux is not significant compared to the radiative one.

3 RESULTS

Varying α_a, α_{DZ} and the viscosity prescription, we obtained a set of disc models listed in Table 1. Models 1–5, 7 and 8 were followed for several thousand orbits of the outer edge of the disc on a grid of 128×32 points in r and θ, respectively. Model 6, which is compared to the analytical description of the disc obtained in Section 4 is computed on a grid with double resolution (256×64). The size of the computational domain was set so that it included a small part of the inner α-disc and a part of the dead zone where the ignitions took place. In radial direction, it was $r = (0.05, 0.35)$ au for Models 1–6, $r = (0.04, 0.3)$ au for Model 7 and $r = (0.1, 0.7)$ au for Model 8. The vertical extent of the computational domain was $\theta = (-5°, 5°)$ for all models. The models are shown in Figs 1 and 2.

Table 1. Parameters of the disc models.

Model	ν type	α_a	α_{DZ}	Grid
1	$\alpha c_s H_a$	10^{-2}	0	128×32
2	$\alpha c_s H_a$	10^{-2}	10^{-4}	128×32
3	$\alpha c_s H_a$	10^{-2}	10^{-3}	128×32
4	$\alpha c_s^2/\Omega$	10^{-2}	0	128×32
5	$\alpha c_s^2/\Omega$	10^{-2}	10^{-4}	128×32
6	$\alpha c_s^2/\Omega$	10^{-2}	10^{-3}	256×64
7	$\alpha c_s^2/\Omega$	5×10^{-3}	5×10^{-4}	128×32
8	$\alpha c_s^2/\Omega$	2×10^{-2}	2×10^{-3}	128×32

3.1 Model 1 ($\nu = \alpha c_s H_a$, $\alpha_a = 10^{-2}$, $\alpha_{DZ} = 0$)

This model is the same as the one described in Paper I, but the current resolution is two times lower. The main purpose of this calculation was to check if we recover all essential features and time-scales observed and measured in Paper I, which is indeed the case. The model develops a strong instability, which quickly leads to the formation of well-separated rings, most of which remain stable for at least a few 100 yr. However, they would probably decay in three-dimensional due to the hydrodynamic instability discovered by Papaloizou & Pringle (1985) as noted in Paper I.

Paper I contains a detailed discussion of the ring instability mechanism. Here we only mention that the key element of that mechanism is the coupling between the changes of the dead zone thickness and the mass-accumulation rate. It turns out that the accretion rate drops at the inner edge of the ring, which works as a bottleneck in the accretion flow along the active surface layer. As a consequence, matter accumulates preferably in the ring.

Since only a small amount of mass flows from the ring inwards, the growth of a given ring is substantially slowed down when additional rings are formed further away from the centre of the disc. If several rings are simultaneously present in the grid, the accretion rate (always measured at the inner boundary of the computational domain) drops to a value as low as $\sim 3 \times 10^{-9} \, M_\odot \, \text{yr}^{-1}$. As the ring accretes mass and becomes denser, its central temperature increases. Once it exceeds T_{lim}, the ring ignites and a 'mini-outburst' ensues, after which the ring is rebuilt at the same position. The accretion rate onto the star increases up to to approximately $5 \times 10^{-9} \, M_\odot \, \text{yr}^{-1}$ during an ignition of a single innermost ring (at $t = 80$ and 220 yr). Moreover, two cases of 'induced ignition' are observed at $t = 490$ and 680 yr. In such a case the heat produced by the ignition and accretion of a particular ring is transported by the radiation to the neighbour rings and makes them active. The accretion rate onto the star increases up to 1.4 and $1.0 \times 10^{-8} \, M_\odot \, \text{yr}^{-1}$.

3.2 Model 2 ($\nu = \alpha c_s H_a$, $\alpha_a = 10^{-2}$, $\alpha_{DZ} = 10^{-4}$)

This model evolves very similarly to Model 1. The non-zero viscosity in the dead zone causes the temperature inside the rings to increase faster, and the induced ignition occurs earlier than in Model 1. The accretion rate in both quiet and ignited states is almost the same as in Model 1.

3.3 Model 3 ($\nu = \alpha c_s H_a$, $\alpha_a = 10^{-2}$, $\alpha_{DZ} = 10^{-3}$)

In this model, we also observe the tendency toward ring formation. However, the viscosity in the dead zone is now sufficiently high to prevent it from splitting. The behaviour characteristic of the rings in Models 1 and 2 is now observed in the whole low-viscosity

area: as the surface density of the disc grows, the temperature at the mid-plane grows as well, and ignition occurs once it exceeds T_{lim}. The accretion rate is increased to $\sim 1.3 \times 10^{-8} \, M_\odot \, \text{yr}^{-1}$, the accumulated mass is quickly removed from the ignited region and the layered structure is re-established. Such mini-outbursts repeat on a time-scale of 100–200 yr. They are not strictly periodic, since the surface density of the layered part of the disc is not completely smooth, as it is incessantly perturbed by the ring instability. At $t = 700$ yr, the whole dead zone contained in the computational domain is ignited and the accretion rate increases up to $4.7 \times 10^{-8} \, M_\odot \, \text{yr}^{-1}$. Since the mini-outburst is stopped by the outer boundary, and the peak accretion rate is probably underestimated.

3.4 Model 4 ($\nu = \alpha c_s^2/\Omega$, $\alpha_a = 10^{-2}$, $\alpha_{DZ} = 0$)

Simulation that produced Model 1 is now repeated with the modified viscosity prescription. Since in the modified prescription there is no direct connection between the thickness of the active layer and the viscosity coefficient, the ring instability needs much more time to develop. The growth rate of the instability is approximately one order of magnitude lower than in Model 1. By the end of the simulation only, the innermost ring is separated from the dead zone, while the remaining ones are visible only as density enhancements within the dead zone. No ignition events are observed. The radial extent of the innermost ring is approximately twice as big as the one in Model 1, and its mass is $5 \times 10^{-6} \, M_\odot$ (approximately five times more than in Model 1).

3.5 Model 5 ($\nu = \alpha c_s^2/\Omega$, $\alpha_a = 10^{-2}$, $\alpha_{DZ} = 10^{-4}$)

This model differs from Model 2 in the same way as Model 4 from Model 1, i.e. only in the formula employed to describe the viscosity. With the modified formula the residual viscosity in the formally dead area is high enough to prevent the formation rings before the dead zone ignites at ~ 700 yr. As a result of ignition the accretion rate increases 5×10^{-9} to $3 \times 10^{-8} \, M_\odot \, \text{yr}^{-1}$. This mini-outburst involves the whole dead zone in the computational domain, so the peak accretion rate is probably underestimated, as in the case of Model 3. Approximately $5 \times 10^{-6} \, M_\odot$ were accreted onto the star during this mini-outburst.

3.6 Model 6 ($\nu = \alpha c_s^2/\Omega$, $\alpha_a = 10^{-2}$, $\alpha_{DZ} = 10^{-3}$)

In this case, the high viscosity in the dead zone completely suppresses the ring instability and the surface density remains smooth in the layered region. Recurrent ignitions and replenishments of the dead zone lead to the periodic oscillations of its inner boundary. The period of these oscillations is around 30 yr. Since the mass accumulates in the whole dead zone, a progressively larger part of it is ignited at each oscillation, and the amplitude of the oscillations generally increases. This increase is accompanied by a slow secular increase of the accretion rate at the inner boundary (from 1×10^{-8} in the beginning to $1.3 \times 10^{-8} \, M_\odot \, \text{yr}^{-1}$ at 364 yr). After each ignition the accretion rate temporarily increases by approximately 10 per cent.

3.7 Model 7 ($\nu = \alpha c_s^2/\Omega$, $\alpha_a = 5 \times 10^{-3}$, $\alpha_{DZ} = 5 \times 10^{-4}$)

The model evolves similarly to Model 6. The accretion rate slowly grows from 2×10^{-9} in the beginning to $5.5 \times 10^{-9} \, M_\odot \, \text{yr}^{-1}$ at $t = 600$ yr. The relative changes during mini-outbursts are slightly higher, reaching approximately 30 per cent. At $t = 400$ yr, a strong
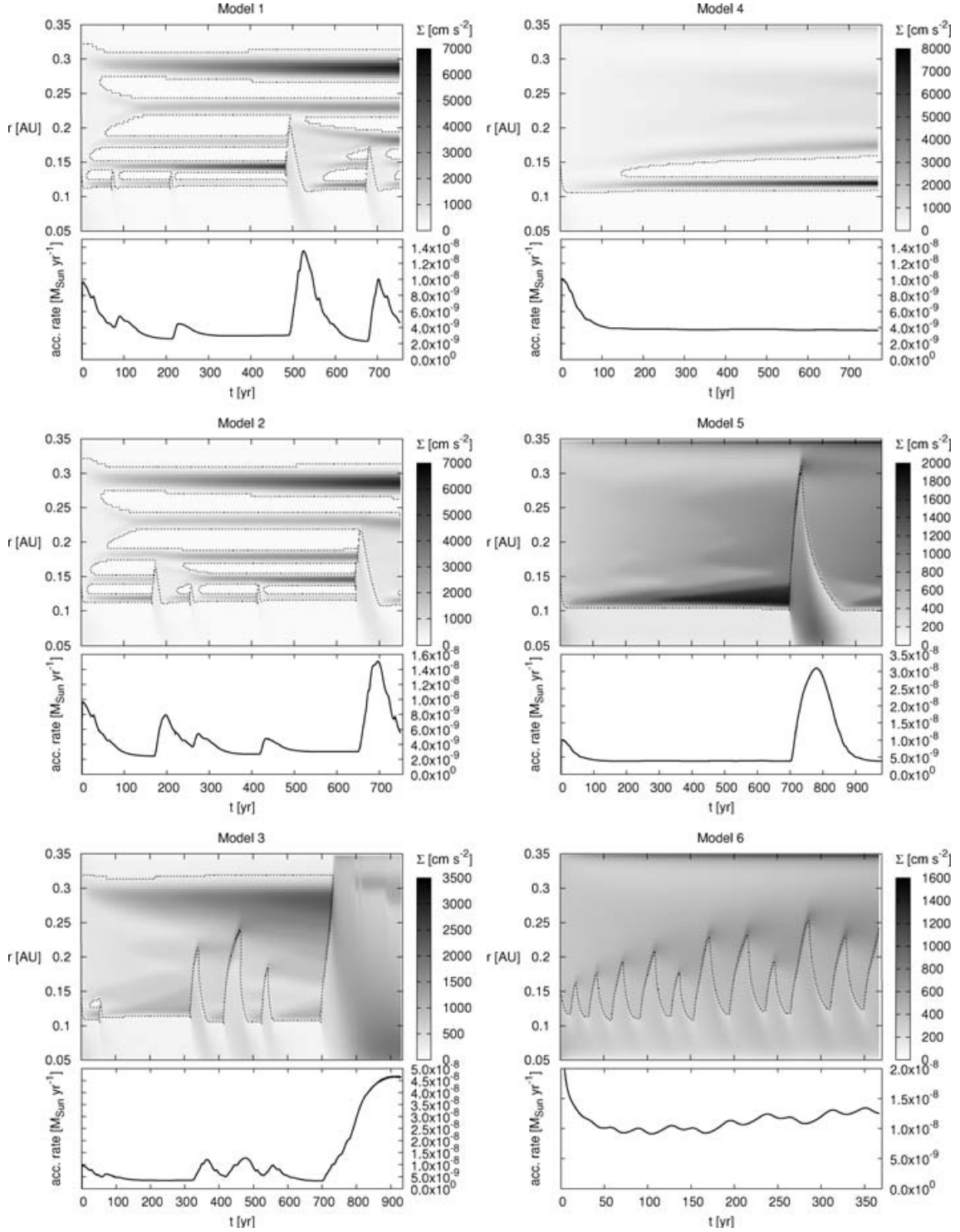
Figure 1. Models 1–6: the top figures show the evolution of the disc surface density (levels of grey), the dashed line denotes the boundary between the dead zone and the active parts of the disc in the mid-plane. The bottom figures show the accretion rate at the inner boundary of the computational domain.

convection occurs in the inner α-disc which makes the accretion-rate curve noisy.

3.8 Model 8 ($\nu = \alpha c_s^2/\Omega$, $\alpha_a = 2 \times 10^{-2}$, $\alpha_{DZ} = 2 \times 10^{-3}$)

This model exhibits very regular mini-outbursts with period $\sim$150 yr. The accretion rate at the inner boundary changes from

2×10^{-8} in the quiet state to the peak value $6 \times 10^{-8}\,\mathrm{M_\odot}\,\mathrm{yr}^{-1}$. The amplitude of the oscillations remains constant, however, double mini-outbursts occur at later stages of the evolution (starting at 1300 yr). The time separation of the two peaks in such double mini-outburst is approximately 50 yr. The outer part of the dead zone is not affected by the oscillations – it remains stationary (see Section 4.1).
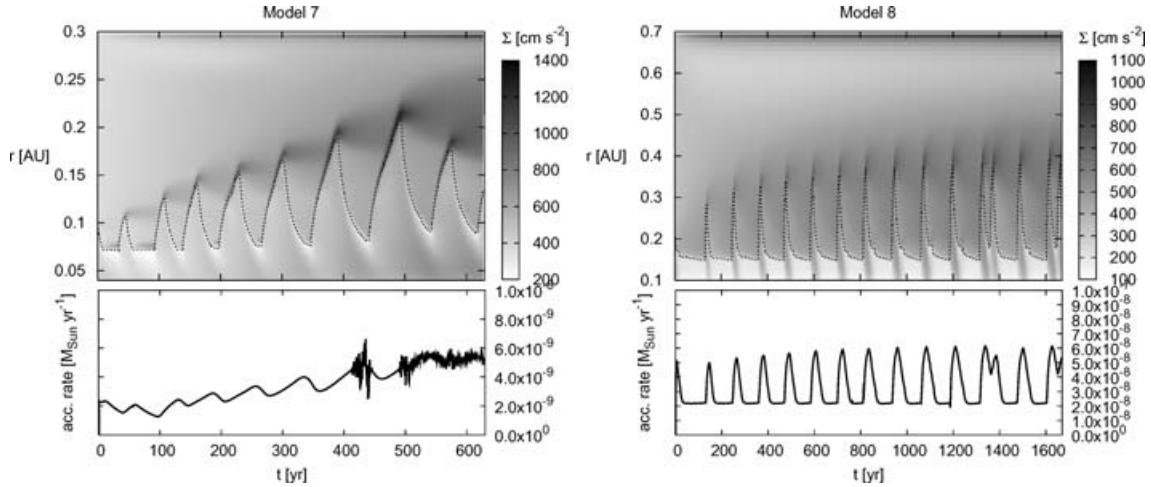
Figure 2. Models 7 and 8. As in Fig. 1.

3.9 Summary

In general, the numerical models exhibit two most remarkable phenomena. If $\alpha_{DZ} = 0$ (Models 1 and 4), the dead zone tends to split into rings. On the other hand, if $\alpha_{DZ} = 0.1 \, \alpha_a$ (Models 3 and 6–8), the dead zone remains unsplit, but the inner boundary of the dead zone starts to oscillate. The mass accumulated in this part of the dead zone is periodically depleted. These oscillations are accompanied by the variations in the accretion rate in the inner active disc. Models 2 and 5 (where $\alpha_{DZ} = 0.01 \, \alpha_a$) are the transitions between the two cases.

Since the ring instability observed in Models 1 and 4 (and partially also 2 and 5) was described in detail in Paper I, in the following we concentrate on the description and explanation of the oscillations.

4 OSCILLATIONS OF THE INNER BOUNDARY OF THE DEAD ZONE

If $\alpha_{DZ} \neq 0$, some accretion in the dead zone occurs. However, as long as the accretion in the active layers dominates, the accretion rate is, in general, a function of radius. It leads to the accumulation of the mass and the growth of the dead zone surface density $2\Sigma_{DZ}$ at a rate

$$2\dot{\Sigma}_{DZ} = \frac{1}{2\pi r}\frac{\partial \dot{M}}{\partial r}, \tag{3}$$

where $\dot{M}$ is the r-dependent accretion rate given by the momentum conservation law

$$\dot{M} = 12\pi r^{1/2}\frac{\partial}{\partial r}\left(\nu_a\Sigma_a + \nu_{DZ}\Sigma_{DZ}\right), \tag{4}$$

where Σ_a, ν_a and ν_{DZ} are surface density of the active layer, viscosity in the active layer and in the dead zone, respectively. Following the standard approach of vertically averaging, we assume the viscosities in forms

$$\nu_{a,DZ} = \alpha_{a,DZ}\frac{c_{s,m}^2}{\Omega}, \tag{5}$$

where $c_{s,m} \equiv (k_B\,T_m)/(\mu m_H)$ is the sound speed in the mid-plane of the disc.

The vertical temperature profile of a disc with z-dependent dissipation rate was obtained by Hubeny (1990). In an optically thick approximation, it can be written as

$$T^4(m) = \frac{3}{4}T_e^4\left[\tau(m) - \tau_\theta(m)\right] \tag{6}$$

using a mass–depth coordinate $m = \int_z^\infty \rho\,\mathrm{d}z'$ changing from 0 (at the disc surface) to $\Sigma/2$ (at the mid-plane). $\tau(m)$ is the optical depth and

$$\tau_\theta(m) = \int_0^m \kappa(m')\theta(m')\,\mathrm{d}m' \tag{7}$$

is the viscosity-weighted optical depth, where

$$\theta(m) = \int_0^m \frac{\nu(m')\,\mathrm{d}m'}{\nu_a\Sigma_a + \nu_{DZ}\Sigma_{DZ}} \tag{8}$$

is the viscosity weight – a monotonically increasing function between $\theta(0) = 0$ and $\theta(\Sigma/2) = 1$. In our model, it assumes the form

$$\theta(m) = \begin{cases} \dfrac{\nu_a m}{\nu_a\Sigma_a + \nu_{DZ}\Sigma_{DZ}} & \text{for} \quad (0, \Sigma_a), \\[2ex] \dfrac{\nu_a\Sigma_a + \nu_{DZ}(m - \Sigma_a)}{\nu_a\Sigma_a + \nu_{DZ}\Sigma_{DZ}} & \text{for} \quad (\Sigma_a, \Sigma/2). \end{cases} \tag{9}$$

The effective temperature, T_e, is given by the formula

$$T_e = \frac{9}{4\sigma}\Omega^2\left(\Sigma_a\nu_a + \Sigma_{DZ}\nu_{DZ}\right), \tag{10}$$

where σ is the Stefan–Boltzmann constant, Ω is the Keplerian angular velocity. Using equations (6)–(9) and (5), we can express the mid-plane temperature $T_m \equiv T(\Sigma/2)$ as

$$T_m^4 = \frac{3}{8}\kappa T_e^4 \frac{\alpha_a\Sigma_a^2 + \alpha_{DZ}\Sigma_{DZ}(\Sigma_{DZ} + 2\Sigma_a)}{\alpha_a\Sigma_a + \alpha_{DZ}\Sigma_{DZ}}\,. \tag{11}$$

Further, we assume that the opacity is a piecewise power-law function of temperature, $\kappa = \kappa_0 T_m^b$, where the coefficients κ_0 and b for different temperature ranges are taken from Bell & Lin (1994). Inserting equation (11) into (4), we obtain a formula for the accretion rate of the layered disc:

$$\dot{M} = 12\pi \left(\frac{27\kappa_0}{32\sigma}\right)^{\frac{1}{3-b}} \left(\frac{k_B}{\mu m_H}\right)^{\frac{4-b}{3-b}} r^{1/2}$$

$$\times \frac{\partial}{\partial r}\left\{\Omega^{\frac{-2+b}{3-b}} r^{1/2}\left(\alpha_a\Sigma_a + \alpha_{DZ}\Sigma_{DZ}\right)\right.$$

$$\left.\times \left[\alpha_a\Sigma_a^2 + \alpha_{DZ}\Sigma_{DZ}\left(\Sigma_{DZ} + 2\Sigma_a\right)\right]^{\frac{1}{3-b}}\right\}, \tag{12}$$

which will be used in Section 4.1.

As more and more mass accumulates in the dead zone, the mid-plane temperature of the disc grows and when it reaches T_{lim} the disc is made active. We can estimate the surface density at the moment of ignition, Σ_{ign}, by substituting T_{lim} for T_m in equation (11) and using a metal-grains-dominated opacity with $\kappa_0 = 0.1$ and $b = 0.5$ (appropriate for temperatures between 203 and $2290\rho^{2/49}$ K). We get

$$\Sigma_{ign} = 2 \left(\frac{320\sigma}{27} \frac{\mu m_H}{k_B \Omega \alpha_{DZ}} T_{lim}^{5/2} - \frac{\alpha_a - \alpha_{DZ}}{\alpha_{DZ}} \Sigma_a^2 \right)^{1/2}. \tag{13}$$

On the other hand, there is a minimum surface density Σ_{mtn} necessary to maintain the disc active. It is the surface density at which the mid-plane temperature of a fully active disc (i.e. of a disc in which the dead zone vanishes) is equal to T_{lim}. We estimate it with the help of the standard α-disc solution, in which the mid-plane temperature $T_{m,\alpha}$ and the effective temperature $T_{e,\alpha}$ obey the relation

$$T_{m,\alpha}^4 = \frac{3}{8} \tau T_{e,\alpha}^4, \tag{14}$$

where $\tau = \kappa \Sigma / 2$ is the optical depth at the mid-plane. In the same solution, the effective temperature is explicitly given by

$$T_{e,\alpha} = \left(\frac{9}{8\sigma} \Sigma \nu_a \Omega^2 \right)^{1/4}. \tag{15}$$

Combining equations (14) and (15) with the opacity formula, we get

$$\Sigma_{mtn} = \left(\frac{1280\sigma \mu m_H}{27 k_B \alpha_a \Omega} \right)^{1/2} T_{lim}^{5/4}. \tag{16}$$

The inner boundary of the dead zone oscillates for reasons explained in Fig. 3. Σ_{ign} and Σ_{mtn} intersect at R_i defined by Gammie as the inner boundary of the dead zone – radius at which limit layered disc with $\Sigma_{DZ} = 0$ has the mid-plane temperature T_{lim}

$$R_i = \left(\frac{27 k_B \alpha_a}{320\sigma \mu m_H} \right)^{2/3} (GM)^{1/3} \Sigma_a^{4/3} T_{lim}^{-5/3}. \tag{17}$$
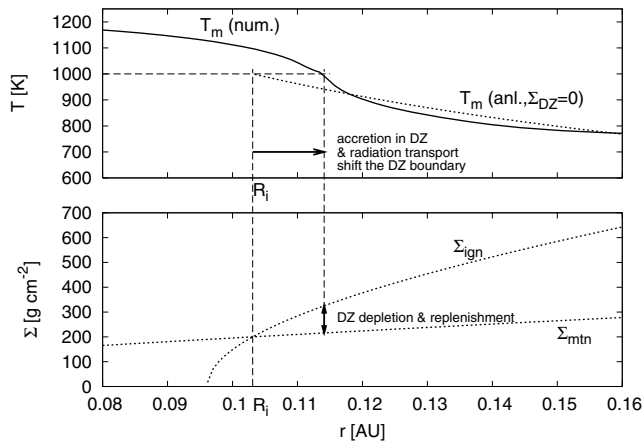
Figure 3. The mechanism of the oscillations of the inner boundary of the dead zone. Top: the mid-plane temperature of the numerical model compared to the analytical one calculated for a disc with the empty dead zone (i.e. $\Sigma_{DZ} = 0$). Bottom: the profiles of Σ_{ign} and Σ_{mtn}. During mini-outbursts the surface density in the inner part of the dead zone oscillates between these two curves.
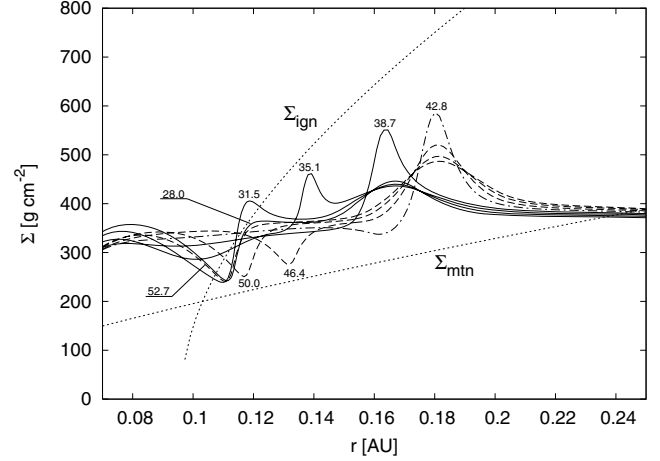
Figure 4. A time sequence of surface-density profiles during the mini-outburst in Model 6 that occurs between 28 and 53 yr. Solid lines (28–38.7 yr): the boundary of the dead zone receding from the star; dot–dashed line (42.8 yr): the boundary has reached the maximum distance from the star; dashed lines (46.4–52.7 yr): the boundary approaches the star.

In numerical models, however, the inner boundary of the dead zone is shifted outwards with respect to R_i. This is because of two effects that increase the temperature in the inner part of the layered disc: the radiation transfer from the adjacent hotter active disc (see also footnote in Gammie 1996); and the residual viscous dissipation in the dead zone.

As soon as the surface density Σ exceeds Σ_{ign}, the dead zone is ignited. The ignition always occurs at the inner boundary of the dead zone, because $\dot{\Sigma}_{DZ}$ is the highest there (it can be shown by solving equation 3 numerically) and Σ_{ign} is an increasing function of the radius. Therefore, the dead zone is ignited from inwards.

In the ignited area the increasing viscosity causes temperature and accretion rate to grow. The radiation flux from the ignited region heats up and ignites the adjacent annulus of the dead zone, so that the active area spreads outwards. On the other hand, the increasing accretion rate tends to decrease the surface density of the ignited region, since the mass is transported from the outer disc at a constant rate independent on whether the dead zone has ignited or not. When Σ drops below Σ_{mtn}, the ignited region becomes dead, the layered structure is re-established and the accumulation of mass starts again. This process is illustrated in Fig. 4 which shows a time sequence of surface-density profiles during one such 'mini-outburst' observed in the numerical model. As one might expect, this behaviour is qualitatively similar to changes in the surface-density profile of discs in cataclysmic variables (CVs) during an outburst; see e.g. Mineshige & Osaki (1985). However, while in CVs two types of outbursts occur (outside–in and inside–out), only the latter seems to be possible in layered discs. As we already mentioned, this is because at smaller radii the surface density of the dead zone increases faster. In principle, it is conceivable that an outburst might produce a density profile with which the next ignition would occur away from the inner edge. We cannot entirely exclude such possibility, although in our simulations, covering a few hundred outbursts in total, such a case has never been observed.

4.1 Stationary solution

The surface density of the dead zone evolves according to equation (3). As Σ_{DZ} grows and the accretion in the dead zone becomes

more and more important, the accumulation rate $\dot{\Sigma}_{DZ}$ decreases. At larger radii, a stationary state with radially constant accretion rate may be reached.

We search for the stationary surface-density profile Σ_{stat} by solving equation (3) numerically with a 1D code similar to that described in Stepinski (1999) and Armitage et al. (2001). The computational domain (0.1–10 au) is divided into 500 cells equidistantly, and the surface density Σ is set to some initial value (e.g. $2\Sigma_a$). Then, the the mid-plane temperature is calculated from equation (11) for every grid cell and it is checked if the cell belongs to the layered part of the disc (if $T_m < T_{\text{lim}}$ and $\Sigma > 2\Sigma_a$) or to the standard α-disc (otherwise). In the the later case, the temperature is recomputed according to equation (14) to obtain the consistent α-disc solution there.

The opacity coefficients κ_0 and b are determined using the first three Bell & Lin regimes only since the analytical solution does not always exist for the remaining ones (i.e. we take into account ice-dominated opacity with $\kappa_0 = 2 \times 10^{-4}$ and $b = 2$ below 167 K, the jump due to ice evaporation with $\kappa_0 = 2 \times 10^{16}$ and $b = -7$ between 167 and 203 K, and metal-grains-dominated opacity with $\kappa_0 = 0.1$ and $b = 0.5$ between 203 and $2290\rho^{2/49}$ K). Our opacity formula may be incorrect for the part of the inner α-disc (and, occasionally, also for the several cells of the layered region where the temperature exceeds $2290\rho^{2/49}$ K). However, using this toy model, we are not particularly interested in the very inner disc, which is much better described by the TRAMP simulation anyway. Moreover, recent works on opacity in protoplanetary discs (see e.g. Semenov et al. 2003) show that the metal grains evaporate at a slightly higher temperature than that adopted by Bell & Lin (1994).

Subsequently, the accretion rate $\dot{M}$ is computed at the boundaries of each cell from equation (12) for the layered disc or from

$$\dot{M}_\alpha = 3\pi\nu_a\Sigma \tag{18}$$

for the α-disc. Finally, the amount of mass proportional to some small time-step dt is transported between cells and Σ is updated. The accretion rate $\dot{M}_{OB}$ at the outer boundary of the domain is a free parameter, and a free outflow condition is imposed at the inner boundary. The computation ends when the accretion rate throughout the computational domain converges to $\dot{M}_{OB}$, i.e. when the stationary state is reached. Typically, it happens after several times 10^5 yr depending on $\dot{M}_{OB}$.

The stationary layered disc surface-density profiles Σ_{stat} for $\dot{M} = 10^{-8}, 10^{-7}$ and 10^{-6} are shown in Fig. 5. They end at the radius R_1 where they cross Σ_{ign} curve, since the stationary layered disc solution does not exist below R_1. The radius R_2 at which Σ_{stat} curve crosses Σ_{mtn} is another distinctive point: it separates the region of the dead zone which after the ignition is able to maintain the temperature above T_{lim} from the one which is not. The dead zone ends at radius R_i where the surface density drops below $2\Sigma_a$.

In this manner, the dead zone can be divided into three parts: (a) the non-stationary periodically depleted and replenished part between R_i and R_1, (b) the stationary, but 'combustible' part between R_1 and R_2 and (c) the stationary 'incombustible' part between R_2 and R_0.

An upper limit for the mass accreted during one mini-outburst in region (a) can be obtained by integration the difference between Σ_{ign} and Σ_{mtn} curves there

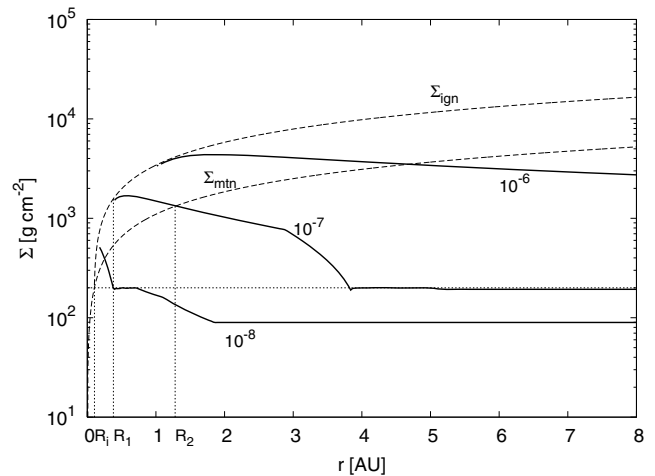$$M_a = 2\pi \int_{R_i}^{R_1} r(\Sigma_{\text{ign}} - \Sigma_{\text{mtn}}) \, dr. \tag{19}$$

Figure 5. The stationary profiles of the surface density for different accretion rates at the inner boundary. The sharp changes of slopes are due to switching between different opacity regimes at temperatures 203 and 167 K. The dashed lines show Σ_{ign} and Σ_{mtn}; the horizontal dotted line denotes a value of $2\Sigma_a$. The distinctive points R_i, R_1 and R_2 for $\dot{M} = 10^{-7}$ M$_\odot$ yr^{-1} model are denoted by the vertical dotted lines.

Taking values R_1 from the numerical model $R_1 = 0.15, 0.38$ and 0.96 au for $\dot{M} = 10^{-8}, 10^{-7}$ and 10^{-6} M$_\odot$ yr^{-1}, respectively, we get

$$M_a \approx \begin{cases} 7.2 \times 10^{-7}\,\text{M}_\odot & \text{for } \dot{M} = 10^{-8}\,\text{M}_\odot\,\text{yr}^{-1}, \\ 2.6 \times 10^{-5}\,\text{M}_\odot & \text{for } \dot{M} = 10^{-7}\,\text{M}_\odot\,\text{yr}^{-1}, \\ 5.2 \times 10^{-4}\,\text{M}_\odot & \text{for } \dot{M} = 10^{-6}\,\text{M}_\odot\,\text{yr}^{-1}. \end{cases} \tag{20}$$

The amount of mass available for the accretion in the region (b) may be interesting in relation to FU Ori-type outbursts. It can be determined as

$$M_b = 2\pi \int_{R_1}^{R_2} r(\Sigma_{\text{stat}} - \Sigma_{\text{mtn}}) \, dr. \tag{21}$$

Integrating numerically the stationary solutions obtained by 1D model, we get

$$M_b \approx \begin{cases} 2.0 \times 10^{-6}\text{M}_\odot & \text{for } \dot{M} = 10^{-8}\,\text{M}_\odot\,\text{yr}^{-1}, \\ 2.7 \times 10^{-4}\text{M}_\odot & \text{for } \dot{M} = 10^{-7}\,\text{M}_\odot\,\text{yr}^{-1}, \\ 0.01\text{M}_\odot & \text{for } \dot{M} = 10^{-6}\,\text{M}_\odot\,\text{yr}^{-1}. \end{cases} \tag{22}$$

The typical amount of mass accreted during the FU Ori-type outburst is ~ 0.01 M$_\odot$ (Hartmann & Kenyon 1996) which is comparable to the mass stored and available for the accretion in the dead zone in the case with $\dot{M} = 10^{-6}$ M$\odot$ yr^{-1}.

5 DISCUSSION

The 2D radiation-hydrodynamic simulations of the layered disc we carried out showed that the behaviour of the disc strongly depends on the presence of a small residual viscosity in the dead zone α_{DZ}. In the models with $\alpha_{DZ} = 0$, the ring instability develops as described in Paper I. The rings may eventually decay which would temporarily increase the accretion rate onto the central star by a factor of several. On the other hand, in the models with α_{DZ} set to 10 per cent of the viscosity in the active parts of the disc, the dead zone remains contiguous, but its inner boundary oscillates.

These oscillations are more or less regular with period between several tens and several hundreds years depending on model parameters. They can be accompanied by variations of the accretion rate on a time-scale as short as 10 yr, at a relative amplitude reaching from a few per cent to 200–300 per cent in the high viscosity Model 8. These variations would be rather difficult to observe, however, it does not seem absolutely impossible. Since the properties of these oscillations are quite sensitive to physical conditions in the disc, such observations could help to constrain the set of models of protoplanetary discs.

Similar variations of the accretion rate were also found by Stepinski (1999) using an 1D hydrodynamic code. However, the period was much longer than in our model (10^3–10^4 yr). The reason for that may be that in his models the ignition of the inner part of the dead zone is much more difficult due to the absence of the radiation transport (and, generally speaking, due to oversimplified description of the interactions between the inner hot α-disc and the layered region).

We give an analytical description of these oscillations based on the vertically averaged model modified for the case of layered disc. It illustrates the mechanism of the dead zone oscillations and tests the numerical model.

Finally, we perform a simple 1D model of the layered disc based on the analytical solution to follow the evolution of the whole layered region for a long time. We found that with $\alpha_{DZ} \neq 0$ a stationary layered region may exist at higher radii (this was also observed in numerical Model 8). Part of this stationary region is still combustible, i.e. it may be made active by increasing the temperature by some external event, and part of its mass is available for accretion.

We compare the amount of mass stored in the combustible region to the mass accreted during a FU Ori-type outburst following the idea that the dead zone can serve as a mass reservoir for such event. We found that these masses are comparable for the case of massive disc with the high accretion rate, which is in agreement with the observation that the FU Ori objects are very young systems.

REFERENCES

Armitage P. J., Livio M., Pringle J. E., 2001, MNRAS, 324, 705
Balbus S. A., Hawley J. F., 1991a, ApJ, 376, 214 (MRI)
Balbus S. A., Hawley J. F., 1991b, ApJ, 376, 223 (MRI)
Bell K. R., Lin D. N. C., 1994, ApJ, 477, 987
Cannizzo J. K., 2001, ApJ, 556, 847
Fleming T., Stone J. M., 2003, ApJ, 585, 908
Fromang S., Terquem C., Balbus S. A., 2002, MNRAS, 329, 18
Gammie C. F., 1996, ApJ, 457, 355
Glassgold A. E., Najita J., Igea J., 1997, ApJ, 480, 344
Hartmann L., Kenyon S. J., 1996, ARA&A, 34, 207
Hawley J. F., Gammie C. F., Balbus S. A., 1995, ApJ, 440, 742
Hubeny I., 1990, ApJ, 351, 632
Klahr H. H., Henning T., Kley W., 1999, ApJ, 514, 325
Kley W., Lin D. N. C., 1999, ApJ, 518, 833
Lodato G., Clarke C. J., 2004, MNRAS, 353, 841
Meyer F., Meyer-Hofmeister E., 1981, A&A, 104, L10
Mineshige S., Osaki Y., 1985, PASJ, 37, 1
Papaloizou J. C. B., Pringle J. E., 1985, MNRAS, 213, 799
Semenov D., Henning Th., Helling Ch., Ilgner M., Sedlmayr E., 2003, A&A, 410, 611
Shakura N. I., Sunyaev R. A., 1973, A&A, 24, 337
Stepinski T., 1999, 30th Annual Lunar and Planetary Science Conference. LPI, Houston, p. A1205
Stone J. M., Hawley J. F., Gammie C. F., Balbus S. A., 1996, ApJ, 463, 656
Umebayashi T., 1983, Prog. Theor. Phys., 69, 480
Umebayashi T., Nakano T., 1981, PASJ, 33, 617
Wünsch R., Klahr H. H., Różyczka M., 2005, MNRAS, 362, 361 (Paper I)

This paper has been typeset from a TEX/LATEX file prepared by the author.